

## Fine structure of negative ions of alkaline-earth-metal atoms

V. A. Dzuba

*Institute of Nuclear Physics, Novosibirsk 630090, U.S.S.R*

V. V. Flambaum

*Institute of Nuclear Physics, Novosibirsk 630090, U.S.S.R*

*and Joint Institute for Laboratory Astrophysics, University of Colorado and National Institute of Standards and Technology, Boulder, Colorado 80309-0440*

G. F. Gribakin

*Leningrad State Technical University, Leningrad 195251, U.S.S.R.*

D. P. Sushkov

*Institute of Nuclear Physics, Novosibirsk 630090, U.S.S.R*

(Received 8 April 1991)

Fine-structure intervals  $np_{1/2}$ - $np_{3/2}$  ( $np_{1/2}$  is the ground state) are calculated for negative ions using relativistic many-body perturbation theory:  $\text{Ca}^-$   $4p$ ,  $56 \text{ cm}^{-1}$ ;  $\text{Sr}^-$   $5p$ ,  $178 \text{ cm}^{-1}$ ;  $\text{Ba}^-$   $6p$ , about  $460 \text{ cm}^{-1}$ ; and  $\text{Ra}^-$   $7p$ ,  $1341 \text{ cm}^{-1}$ . Comparison of the fine-structure interval with affinity:  $\text{Ca}^-$  10%,  $\text{Sr}^-$  22%,  $\text{Ba}^-$  30%; for  $\text{Ra}^-$  the fine-structure interval is larger than the affinity. Thus the  $\text{Ra}^-$   $7p_{3/2}$  state is a resonance in the continuous spectrum with energy 0.018 eV. This means that the relativistic spin-orbit interaction plays a determining role in slow electron-radium scattering.

### I. INTRODUCTION

Recently, calculations of negative ions of alkaline-earth-metal atoms Ca, Sr, Ba, and Ra have been carried out [1–6]. These calculations have shown that these atoms have positive affinity and stable negative ions with configuration  $ns^2np$ . This supports the experimental discovery [7] of the first negative ion of this type,  $\text{Ca}^-$ , which was predicted theoretically [8]. The present work is a calculation of the fine structure of alkaline-earth-metal negative ions.

The main feature of these negative ions is that the electron is bound with the atom that has closed subshells. This bond is only due to the strong correlation (polarization) interaction of the extra electron with atomic electrons. This explains the small binding energy  $\sim 0.1 \text{ eV}$ . Therefore, we should accurately take into account both correlation and relativistic (spin-orbit) corrections. The energy of spin-orbit splitting (fine-structure interval)  $\Delta E_{\text{fs}}$  between  $p_{1/2}$  and  $p_{3/2}$  levels is proportional to  $z^2\alpha^2$ , where  $z$  is the nuclear charge,  $\alpha = \frac{1}{137}$ . However, our calculation shows that even for the lightest ion  $\text{Ca}^-$  ( $z=20$ )  $\Delta E_{\text{fs}} = 56 \text{ cm}^{-1}$ , which constitutes 10% of the  $4p$ -electron binding energy. The value of  $\Delta E_{\text{fs}}$  increases rapidly in the row of negative ions  $\text{Ca}^-$ ,  $\text{Sr}^-$ ,  $\text{Ba}^-$ , and  $\text{Ra}^-$ . And for  $\text{Ra}^-$   $7s^27p$ ,  $\Delta E_{\text{fs}}$  is larger than the binding energy of the  $7p_{1/2}$  electron, i.e., the upper fine-structure level  $\text{Ra}^-$   $7p_{3/2}$  lies in the continuous spectrum and is unstable.

In the present work we use relativistic many-body perturbation theory and the correlation potential method to calculate  $np_{1/2}$  and  $np_{3/2}$  energy levels of negative ions

and to find the fine-structure interval  $\Delta E_{\text{fs}} = E_{np_{3/2}} - E_{np_{1/2}}$ .

This method allows us accurately to calculate the correlation interaction of the external electron with the electronic core, which creates the negative-ion bound state. The accuracy of our calculation of the external electron energy level in the usual atoms is  $\sim 1\%$  for Tl [9] and  $\sim 0.1\%$  for Cs [10]. Even though we use the same method, the accuracy for the negative-ion affinity cannot be as good since these very weakly bound levels are very sensitive to the accuracy of correlation correction calculations (1% change of correlation interaction leads to  $\sim 10\%$  change of affinity). Our estimate of accuracy in this case is about 30%. However, the accuracy of the fine-structure interval calculation is much better: a few percent.

We should note that previous calculations of affinity were carried out by the many-configuration Hartree-Fock method [8,3], the Dyson equation in nonrelativistic variant [7,6], and in the relativistic variant [5]. Use of the Dyson equation was suggested in Refs. [11] and [12]; a local-density method was used in Ref. [2], and an  $R$ -matrix theory was used in Ref. [4].

### II. METHOD OF CALCULATION

The energy of the external electron in a negative ion can be found from the single-particle equation (see, e.g., Refs. [2,5,9,10], and references therein):

$$(\hat{H}_0 + \hat{\Sigma})\psi_a = E_a\psi_a, \quad (1)$$

where  $\hat{H}_0$  is the relativistic Hartree-Fock-Dirac Hamiltonian

$$\hat{H}_0 = c\boldsymbol{\alpha} \cdot \mathbf{p} + (\beta - 1)mc^2 - \frac{ze^2}{r} + \hat{V}^N, \quad (2)$$

$\hat{V}^N = V_{\text{dir}} + \hat{V}_{\text{exch}}$  is the Hartree-Fock potential created by the electrons of the neutral atom,  $V_{\text{dir}}$  and  $\hat{V}_{\text{exch}}$  are direct and nonlocal exchange potentials, and  $\hat{\Sigma}$  is the nonlocal correlation potential (integration operator) created by the electrons of the neutral atom:

$$\hat{\Sigma}\psi_a = \int \Sigma(\mathbf{r}_1, \mathbf{r}_2, E_a) \psi_a(\mathbf{r}_2) d^3r_2. \quad (3)$$

In terms of many-body theory,  $\hat{\Sigma}$  is a self-energy operator for a single-electron Green function. The calculation of  $\hat{\Sigma}$  is discussed below. We use the caret symbol for nonlocal (integration) operators.

In a neutral atom, Eq. (1) determines the so-called Brückner orbitals  $\psi_a$ . Correlation correction (shift of energy with respect to Hartree-Fock value) is determined by the operator  $\hat{\Sigma}$  and is approximately equal to the first-order correction in  $\hat{\Sigma}$ :  $\langle a | \Sigma | a \rangle$ . Equation (1) also includes higher-order corrections in  $\hat{\Sigma}$ , which, however are small. Thus, in atoms,  $\hat{\Sigma}$  plays the role of a relatively small perturbation.

For negative ions it is impossible to consider  $\hat{\Sigma}$  as a perturbation since the negative ion would be unstable if  $\hat{\Sigma}$  is neglected. Note also, in this case  $\hat{\Sigma}$  is substantially larger than for an electron in a neutral atom. Actually, the long distance asymptotic form of correlation potential ( $r_1, r_2 \gg a_B$ ) is

$$\Sigma(r_1, r_2, E_a) \rightarrow -\frac{\alpha e^2}{2r_1^4} \delta(\mathbf{r}_1 - \mathbf{r}_2). \quad (4)$$

Here,  $a_B$  is the Bohr radius, while  $\alpha$  is electric dipole polarizability. The negative-ion external electron is influenced by the polarizability of the neutral atom, which is much larger than the polarizability of the positive ion that influences an electron in a neutral atom.

In the present work we do the calculations as follows.

(1) The Hartree-Fock-Dirac potential of the neutral atom  $V^N$  and Hamiltonian  $H_0$  are used for a zero approximation basis of states creation (for many-body perturbation theory calculations of  $\hat{\Sigma}$ ).

(2) The correlation potential  $\Sigma(\mathbf{r}, \mathbf{r}_2, E_a)$  in the  $p_{1/2}$  and  $p_{3/2}$  partial waves is calculated.

(3) Equation (1) is solved for  $np_{1/2}$  and  $np_{3/2}$  orbitals and the fine-structure interval is calculated from

$$\Delta E_{\text{fs}} = E_{np_{3/2}} - E_{np_{1/2}}.$$

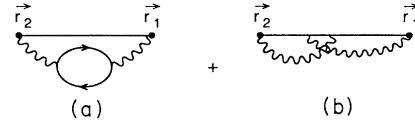


FIG. 1. Second-order diagrams for the correlation potential  $\hat{\Sigma}$ .

Now consider the details of these calculations using as an example the ion  $\text{Ca}^-$ . We use Green functions and Feynman diagram techniques to calculate  $\hat{\Sigma}$ . (Corresponding methods of Green-function and diagram calculations are described in Refs. [9], [10], and [14].) Usage of these techniques is convenient for the summation of high-order diagrams and provides better accuracy than direct summation over intermediate states in perturbation theory.

In the lowest- (second-) order in residual electron-electron interactions,  $\hat{\Sigma}$  is described by two diagrams shown in Fig. 1. The detailed results of our calculations for  $\text{Ca}^-$  are presented in Table I. The main contribution to the polarizability of Ca (which determines the asymptotic form of the correlation potential) is given by  $4s^2$  subshell [see column (a), line 4], and is sufficient to take into account the contribution of this subshell only to obtain the negative-ion state. However, the binding energy of the  $4p_{1/2}$  electron in this approximation [column (a)] is essentially smaller than the experimental affinity [column (e)]. Note that it is convenient to find the value of the polarizability using the asymptotic behavior of the polarization operator (Fig. 2):

$$\Pi(\mathbf{r}_1, \mathbf{r}_2, \omega) \approx r_1^{-1} r_2^{-2} \alpha \quad (5)$$

at

$$r_1, r_2 \gg a_B, \quad \omega = 0.$$

The polarization operator is the most essential part of diagram 1(a). In second-order diagrams the value of the polarizability is strongly underestimated ( $\alpha = 120a_B^3$ ; experiment  $\alpha(\text{Ca}) = 170a_B^3$ , Ref. [13]). Inclusion of the  $3p^6$  inner shell of the Ca atom increases the polarizability by  $\alpha + 3a_B^3$  only. However, the binding energy of the  $4p_{1/2}$  electron is doubled [column (b)]. This means that there is no direct connection between the polarizability and power of the correlation potential. In other words, the region inside the atom is essential where asymptotic for-

TABLE I. Binding energies of  $4P_{1/2}$  and  $4P_{3/2}$  states of  $\text{Ca}^- 4s^2 4p$  negative ion. Column (a): Only the second-order contribution of the  $4s$  subshell to  $\hat{\Sigma}$  (Fig. 1) is taken into account; column (b) second-order,  $4s$ , and  $3p$  subshell contribution; column (c)  $4s$  contribution with the particle-hole interaction and screening taken into account; column (d)  $4s$  and  $4p$  contribution with screening and particle-hole interaction; column (e) experiment: binding energy (Ref. [7]) and polarizability (Ref. [13]).

	(a)	(b)	(c)	(d)	(e)
$4P_{1/2}$ (meV)	24.2	55.8	54.5	71.0	$43 \pm 7$
$4P_{3/2}$ (meV)		48.9		64.1	
$\Delta E_{\text{fs}}$ ( $\text{cm}^{-1}$ )		56		56	
$\alpha$ (units of $a_B^3$ )	120	123	149.1	149.8	170

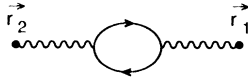


FIG. 2. Polarization operator.

mula (4) is not applicable.

Estimates show that this doubling of the binding energy corresponds to a 10% increase of power of the correlation potential. The strong dependence of the binding energy on the correlation potential power is because the greater part of the correlation potential ( $\sim 80\%$ ) is spent on the creation of the bound state from the continuous spectrum (i.e.,  $0.8\hat{\Sigma}$  gives the bound state with energy  $E = -0$ ) and only a small part determines the position of the level. Thus, we need great accuracy ( $\sim 1\%$ ) in the calculation of  $\hat{\Sigma}$  to obtain the affinity with an accuracy of 10% (in the neutral atom, the situation is just the opposite: a 10% accuracy in  $\hat{\Sigma}$  gives a 1% accuracy in the energy calculation). Therefore, the agreement between the calculated  $4p_{1/2}$  binding energy 55.8 meV ( $\hat{\Sigma}$  calculated in second order) and the experimental value  $43 \pm 7$  meV looks satisfactory. In the same approximation the binding energy of the  $4p_{3/2}$  electron is 48.9 meV, i.e., the fine-structure interval  $\Delta E_{fs} = 6.9$  meV  $\approx 56$  cm $^{-1}$ . This value of  $\Delta E_{fs}$  is comparable with experimental error in the affinity of the Ca atom. If, in experiment, the Ca $^{-}$  ions are created in both the  $4P_{1/2}$  and  $4P_{3/2}$  state, the observed affinity probability corresponds to a statistical average value, which is closer to the  $4P_{3/2}$  energy. In our calculation this value

$$|E| = \left| \frac{1}{3}E_{4P_{1/2}} + \frac{2}{3}E_{4P_{3/2}} \right| = 51.1 \text{ meV} .$$

Consider now the contribution of higher-order diagrams to the correlation potential  $\hat{\Sigma}$ . Our experience shows that for the neutral atom two classes of diagrams are the most important (see Refs. [9] and [10]): the particle-hole interaction in the polarization operator (Fig. 3) and the screening of the electron-electron interaction (Fig. 4). The first effect essentially decreases the energy denominators that appear in the perturbation theory, and correspondingly increases the polarization operator and the correlation potential  $\hat{\Sigma}$ . It is easy to take this effect into account by calculation of the Green function, which enters into the polarization operator (Fig. 2) in the field of atomic core with the hole. Screening of the electron-electron interaction decreases the polarization of the electronic core by the external electron and decreases the correlation potential  $\hat{\Sigma}$ . The method of the screening calculation is described in Refs. [9] and [10]. (This calculation is, in fact, a summation of the matrix geometrical progression for the polarization operator  $\hat{\Pi} = \Pi(r_1, r_2)$  and the Coulomb interaction  $\hat{Q}$ ; it reduces to a calcula-

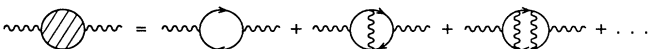


FIG. 3. Particle-hole interaction in the polarization operator.



FIG. 4. Screening of the electron-electron interaction.

tion of an inverse matrix: the renormalized operator is  $\hat{\Pi} = \hat{\Pi}[1 + i\hat{Q}\hat{\Pi}]^{-1}$ .) The final diagrams for  $\hat{\Sigma}$  which include the particle-hole interaction in  $\hat{\Pi}$  and the screening of the electron-electron interaction, are presented in Fig. 5. For simplicity, we neglect higher-order correlations in the exchange diagram in Fig. 5(b) since this diagram is considerably smaller than that in Fig. 5(a), and we do not need high accuracy in its calculation.

The results of this calculation are presented in column (d) of Table I. The effects of the particle-hole interaction in the polarization operator and the screening strongly compensate each other. Therefore, the binding energies of  $4P_{1/2}$  and  $4P_{3/2}$  only slightly exceed the values obtained in the second-order calculation of  $\hat{\Sigma}$  [column (b)]. The fine-structure interval practically does not change. Note that the observed change in the  $4P$  binding energy corresponds to a 4% change of the correlation potential power only. But the new value for the polarizability  $\alpha = 149.8a_B^3$  substantially exceeds the second-order result and lies much closer to the experimental value. This is explained by more accurately taking into account the particle-hole interaction.

It is interesting also that the screening of the electron-electron interaction reduces drastically the polarization of internal shells by the external electron field. In column (c) of Table I we present results that take into account  $4s$  contributions to  $\Sigma$  (Fig. 5) and  $\alpha$  only. Comparison with column (d) shows that screening suppresses the contributions of the  $3p$  shell to the polarizability four times ( $0.7a_B^3$  instead of  $3a_B^3$ ) and the contribution to the  $4P_{1/2}$  binding energy two times. It is easy to understand this fact. The external shell  $4s^2$  drastically screens the field of the extra weakly bound electron inside the atom similar to the screening of an applied electric field by the external atomic shell (see Ref. [15]).

It is interesting to determine how much we overestimate the correlation potential (with the particle-hole interaction and screening taken into account; see Fig. 5). If we introduce the factor 0.932 to  $\hat{\Sigma}$ , we obtain the binding energy of the  $4P_{1/2}$  level 43 meV (remember that the experimental value is  $43 \pm 7$  meV). The overestimation factor would probably be even closer to unity if the statistically averaged energy of  $4P_{1/2}$  and  $4P_{3/2}$  were measured. We see also that we need the  $\hat{\Sigma}$  calculation with 1% accu-

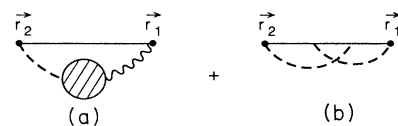
FIG. 5. Diagrams for the correlation potential  $\hat{\Sigma}$  taking into account the particle-hole interaction and the screening of the electron-electron interaction.

TABLE II. Binding energies of  $np_{1/2}$  and  $np_{3/2}$  states and fine-structure intervals for negative ions of rare-earth atoms.

Z	Ion	Binding energy ( $10^{-3}$ eV)		$\Delta E_{fs}$ ( $\text{cm}^{-1}$ )	$np_{1/2}^a$
		$np_{1/2}$	$np_{3/2}$		
20	$\text{Ca}^- 4s^2 4p$	56	49	56	56
38	$\text{Sr}^- 5s^2 5p$	102	80	178	93
56	$\text{Ba}^- 6s^2 6p$			460 <sup>b</sup>	192
88	$\text{Ra}^- 7s^2 7p$	148	-18	1341	125

<sup>a</sup>Other calculations for  $\text{Ca}^-$ ,  $\text{Sr}^-$ ,  $\text{Ba}^-$  (Ref. [5]) and  $\text{Ra}^-$  (Ref. [2]).

<sup>b</sup> $\text{Ba}^-$  fine structure is extrapolated from  $\text{Ra}^-$  and  $\text{Sr}^-$  calculations ( $\Delta E_{fs} \sim Z^2$ ).

racy to obtain affinity with 10% accuracy. Now we have an accuracy of several percent in  $\hat{\Sigma}$  (see Ref. [10]).

### III. RESULTS AND DISCUSSION

The results for  $\text{Ca}^-$  presented above show that the binding energies of the  $4p_{1/2}$  and  $4p_{3/2}$  electron states are very sensitive to the power of the correlation potential  $\hat{\Sigma}$  and depend on the approximation that is used for the calculation of  $\hat{\Sigma}$ . However, the fine-structure interval  $\Delta E_{fs}$  is practically not sensitive. The reason is the following. The matrix element of the spin-orbit interaction is determined mainly by the small region near the nucleus ( $U_{ls} \sim z/r^3$ ). The small distance behavior of the  $p$ -wave function depends slightly on  $\hat{\Sigma}$  since even for energy  $E \rightarrow 0$  a wave function with orbital angular momentum  $l \geq 1$  tends to the quadratically integrable function ( $\psi \sim r^{-l-1}$ ). Therefore, we can calculate the fine-structure interval using the simplest second-order approximation (Fig. 1) and take into account both the external shell and several inner-shell excitations in the polarization operator loop.

The energy of the states  $np_{1/2}$  and  $np_{3/2}$  and the fine-structure intervals for negative ions  $\text{Ca}^- 4p$ ,  $\text{Sr}^- 5p$ , and  $\text{Ra}^- 7p$  calculated in this way are presented in Table II. For comparison, we also present in this table the energies of  $np_{1/2}$  levels for  $\text{Ca}^-$ ,  $\text{Sr}^-$ , and  $\text{Ba}^-$  by solution of the relativistic Dyson equation [5], and for  $\text{Ra}^-$  obtained by the local-density method with relativistic corrections [2]. The correlation potential  $\hat{\Sigma}$  in Ref. [5] was calculated in the second-order of perturbation theory. Our results in Table II were obtained with the same physical approximation. Therefore, the good agreement with the results for  $np_{1/2}$  levels between the present work and Ref. [5] is only the test of computational accuracy [we use different methods of  $\Sigma$  calculations and different methods of the solution of Eq. (1)]. The small difference in the results corresponds to  $\sim 1\%$  accuracy of  $\Sigma$  calculation.

Barium has the largest affinity among these four atoms.

It looks natural since Ba has the largest polarizability ( $\alpha(\text{Ba})=270$ ,  $\alpha(\text{Ca})=170$ ,  $\alpha(\text{Sr})=190$  (see Ref. [13]); for Ra our calculation gives  $\alpha \approx 206a_B^3$ ).

Fine-structure intervals  $\Delta E_{fs}$  rapidly increase with nuclear charge ( $\sim Z^2$ ). Therefore, the  $7p_{3/2}$   $\text{Ra}^-$  level appears in the continuous spectrum at energy  $E_p=0.018$  eV. This quasistationary state of the ion  $\text{Ra}^- 7p_{3/2}$  decays by tunneling through the centrifugal barrier and has a small width:  $\Gamma(E_p)/E_p \approx 0.58$  (note that  $\Gamma \sim E^{3/2}$ ; the calculation of  $\Gamma$  is carried out in our work [17]). In the scattering of low-energy electrons this state appears as a resonance in the  $p_{3/2}$  wave. There is no such resonance in the  $p_{1/2}$  wave. Thus the scattering of electrons on Ra is a wonderful example of how relativistic spin-orbit interaction plays a determining role in the scattering of very slow electrons (for a detailed calculation of corresponding relativistic effects, see Ref. [17]).

The upper  $np_{3/2}$  levels are metastable in  $\text{Ca}^-$ ,  $\text{Sr}^-$ , and  $\text{Ba}^-$  ions. They decay by the  $M1$  transition  $np_{3/2} \rightarrow np_{1/2}$  (the  $E2$  transition is suppressed due to small frequency; even for Ba  $w_{E2}/w_{M1} \lesssim 4 \times 10^{-2}$ ). The probability of an  $M1$  transition is (see, e.g., Ref. [16])

$$w_{M1}(np_{3/2} \rightarrow np_{1/2}) = \frac{\hbar e^2 \omega^3}{9m^2 c^5}. \quad (6)$$

By substituting the frequency  $\omega = \Delta E_{fs}/\hbar$  one obtains lifetimes of  $P_{3/2}$  levels: for  $\text{Ca}^-$ ,  $635 \times 10^3$  s; for  $\text{Sr}^-$ ,  $19.8 \times 10^3$  s; and for  $\text{Ba}^-$ , about  $2.7 \times 10^3$  s. Since the lifetimes are large it is necessary to take into account the existence of a metastable  $np_{3/2}$  level in the affinity measurements.

### ACKNOWLEDGMENTS

The authors are grateful to M. Yu. Kuchiev and V. K. Ivanov for support of this work. One of us (V.V.F.) received support from the visiting fellowship program at the Joint Institute Laboratory Astrophysics (JILA). V.V.F. thanks the staff of the JILA Scientific Reports Office for their assistance in the preparation of this paper.

[1] G. F. Gribakin, B. V. Gul'tsev, V. K. Ivanov, and M. Yu. Kuchiev, Pis'ma Zh. Tekh. Fiz. 15, 32 (1989).

[2] S. H. Vosko, J. B. Lagowski, and J. L. Mayer, Phys. Rev. A 39, 446 (1989).

[3] C. Froese Fischer, Phys. Rev. A 39, 963 (1989).

[4] L. Kim and C. H. Greene, J. Phys. B 22, 175 (1989).

[5] W. R. Johnson, J. Sapirstein, and S. A. Blundell, J. Phys. B 22, 2341 (1989).

- [6] G. F. Gribakin, B. V. Gul'tsev, V. K. Ivanov, and M. Yu. Kuchiev, *J. Phys. B* (to be published).
- [7] D. J. Pegg, J. S. Thompson, R. N. Compton, and G. D. Alton, *Phys. Rev. Lett.* **59**, 2267 (1987).
- [8] C. Froese Fischer, J. B. Lagowski, and S. H. Vosko, *Phys. Rev. Lett.* **59**, 2263 (1987).
- [9] V. A. Dzuba, V. V. Flambaum, P. G. Silvestrov, and O. P. Sushkov, *Phys. Lett. A* **131**, 461 (1988).
- [10] V. A. Dzuba, V. V. Flambaum, and O. P. Sushkov, *Phys. Lett. A* **140**, 493 (1989).
- [11] G. F. Gribakin, V. K. Ivanov, M. Yu. Kuchiev, and L. V. Chernysheva (unpublished).
- [12] L. V. Ghernysheva, G. F. Gribakin, V. K. Ivanov, and M. Yu. Kuchiev, *J. Phys. B* **21**, 419 (1988).
- [13] A. A. Radtzig and B. M. Smirnov, *Parameters of Atoms and Atomic Ions Handbook* (Energoatomizdat, Moscow, 1986, in Russian).
- [14] V. A. Dzuba (unpublished).
- [15] V. A. Dzuba, V. V. Flambaum, P. G. Silvestrov, and O. P. Sushkov, *Phys. Lett. A* **118**, 177 (1986).
- [16] V. B. Berestetzky, E. M. Lifshitz, and P. L. Pitaevsky, *Quantum Electrodynamics* (Nauka, Moscow, 1980).
- [17] V. A. Dzuba, V. V. Flambaum, and O. P. Sushkov, *Phys. Rev. A* (to be published).